PROCEEDINGS A

royalsocietypublishing.org/journal/rspa

Research

**Cite this article:** Morrison LV, Stephenson FR, Hohenkerk CY, Zawilski M. 2021 Addendum 2020 to 'Measurement of the Earth's rotation: 720 BC to AD 2015'. *Proc. R. Soc. A* **477**: 20200776.
https://doi.org/10.1098/rspa.2020.0776

Received: 28 September 2020
Accepted: 18 January 2021

**Subject Areas:**
geophysics, Solar System

**Keywords:**
eclipses, Earth's rotation, length of day

**Author for correspondence:**
L. V. Morrison
e-mail: lmorr49062@aol.com



# Addendum 2020 to 'Measurement of the Earth's rotation: 720 BC to AD 2015'

L. V. Morrison[1], F. R. Stephenson[2], C. Y. Hohenkerk[3] and M. Zawilski[4]

[1]Pevensey, East Sussex, UK; formerly Royal Greenwich Observatory, UK
[2]Department of Physics, University of Durham, Durham, UK
[3]Taunton, Somerset, UK; formerly HM Nautical Almanac Office, UK
[4]IOTA/ES (International Occultation Timing Association/European Section), Poland

CYH, 0000-0002-2883-6606

Historical reports of solar eclipses are added to our previous dataset (Stephenson *et al.* 2016 *Proc. R. Soc. A* **472**, 20160404 (doi:10.1098/rspa.2016.0404)) in order to refine our determination of centennial and longer-term changes since 720 BC in the rate of rotation of the Earth. The revised observed deceleration is $-4.59 \pm 0.08 \times 10^{-22}$ rad s$^{-2}$. By comparison the predicted tidal deceleration based on the conservation of angular momentum in the Sun–Earth–Moon system is $-6.39 \pm 0.03 \times 10^{-22}$ rad s$^{-2}$. These signify a mean accelerative component of $+1.8 \pm 0.1 \times 10^{-22}$ rad s$^{-2}$. There is also evidence of an oscillatory variation in the rate with a period of about 14 centuries.

## 1. Introduction

In a paper by three of the current authors—Stephenson *et al.* [1], herein referred to as paper 2016—a comprehensive compilation was presented of historical reports of solar and lunar eclipses in the period 720 BC to AD 2015, from which we deduced changes in the Earth's rate of rotation. That investigation indicated that there are changes in the rate on centennial as well as decadal time scales. We have pursued this question further by adding new results from solar eclipses in the period 196 BC to AD 1361, which we have published since 2016. Besides these results, we have recently had access to an unpublished archive of medieval European records of solar eclipses in the period AD 840–1597 assembled by

Electronic supplementary material is available online at https://doi.org/10.6084/m9.figshare.c.5300925.

THE ROYAL SOCIETY PUBLISHING

Marek Zawilski. Many of these records have not been analysed before for the purpose of measuring changes in the Earth's rotation.

Total and annular eclipses produce narrow shadow bands on the Earth's surface, with very sharp boundaries. Extant historical records of where and when these eclipses were seen can establish the rotational angle of the Earth at those epochs relative to a fixed celestial frame defined by the apparent orbits of the Sun and Moon. The uncertainty of the angle is determined by the width of the eclipse shadow projected parallel to the equator. Sometimes a report of a large partial eclipse can be used in the inverse sense that the eclipse was not total, but nearly so. Before the advent of the telescope *ca* AD 1600, the observations of solar eclipses are potentially the most accurate way of determining the Earth's rotational phase. The narrowness and sharpness of the shadow mean that timing is not required, which removes the attendant uncertainty involved in determining the local time of the eclipse. Nevertheless, timing of both solar and lunar eclipses can act as a secondary, generally less accurate source of measurement.

We present in the main part of this addendum our updated and new results of untimed solar eclipses and the revision of the results for the centennial variation of the Earth's rotation presented in our 2016 paper [1]. The electronic supplementary material, Supplement gives for each of the new medieval eclipses the track and our analysis of the reports leading to the determination of $\Delta$T.

## 2. Measurement of the parameter $\Delta$T

For each eclipse observation the calculated date, time and position of the umbral/central path is made on the assumption that the rate of rotation of the Earth is constant with respect to the uniform time scale, Terrestrial Time (TT), which is realized from the independent variable in the dynamical equations of motion of the Sun and Moon. A reliable eyewitness account of an eclipse fixes the angular position of the Earth in Universal Time (UT), which is the time scale realized from the variable rotation of the Earth. The difference TT−UT, denoted by $\Delta$T, measures the accumulative error in time due to the variation in the Earth's rate of rotation between an assumed origin in time and the date of the eclipse. The changes in rate of rotation are conventionally measured as changes in the length of the mean solar day (lod) compared with the standard length of 86 400 seconds (s) TAI (International Atomic Time). For historical reasons, owing to the unit of time on the UT scale being defined in terms of the average apparent mean motion of the Sun between AD 1750 and AD 1892, this standard is the lod around the epoch AD 1825 (see [1, §4a]).

For the purposes of calculation, we will hereafter use the algebraic numbering of the year in the Julian/Gregorian calendar rather than the discontinuous BC/AD system, which has no year zero: for example, 198 BC = −197.

## 3. Published results for $\Delta$T since 2016

Morrison *et al.* [2] include a discussion of ancient Chinese records of total and annular solar eclipses in the years −197, +306, +616, +1361, and a European record of +1239. Stephenson *et al.* [3] discuss the Chinese eclipses of +65 and +454, and Morrison *et al.* [4] discuss the total solar eclipse of −187 witnessed in Rome. These published results for $\Delta$T obtained since 2016 are displayed in table 1.

## 4. New results for $\Delta$T for the years +1133 to +1598

Table 2 contains the new results for $\Delta$T obtained from a discussion of the Zawilski archive +840 to +1598. Their derivation is set out in the electronic supplementary material.

**Table 1.** Published bounds on $\Delta T$ (s) since 2016 derived from untimed solar eclipses.

| year | type | upper > ΔT > lower | | places |
|---|---|---|---|---|
| −197 | annular | +13 020 | +6360 | China (Chang'an) |
| −187 | total | +12 900 | +12 590 | Europe (Rome) |
| +65 | total | +8900 | +8450 | China (Luoyang) |
| +65 | total | +9630 | +9150 | China (Guangling) |
| +306 | annular | +7890 | +6550 | China (Luoyang) |
| +454 | total | +7800 | +6030 | China (Jiankang) |
| +616 | annular | +2990 | +2270 | China (Luoyang) |
| +1239 | total | +1020 | +820 | Europe (Cardeña; Toledo) |
| +1361 | total | +1760 | +500 | China (Songjiang) |

**Table 2.** New bounds on $\Delta T$ (s) for the years +1133 to +1598 derived from untimed solar eclipses.

| year | type | upper > ΔT > lower | | places |
|---|---|---|---|---|
| +1133 | total | +1115 | +530 | Kerkrade; Reichersberg |
| +1187 | total | +1065 | +45 | Galich |
| +1239 | total | +1105 | +830 | Cerrato; Toledo |
| +1241 | total | +1005 | +625 | Freising; Stade |
| +1310 | annular | +1555 | +460 | Erfurt; Paris |
| +1330 | partial | +910 | — | Zbraslav |
| +1379 | total | +1525 | +105 | Sevilla |
| +1386 | total | +1075 | −650 | Montpellier |
| +1406 | total | +900 | +400 | Liège; Bordeaux |
| +1415 | total | +705 | +200 | Wrocław; Kraków |
| +1433 | total | +570 | +385 | Augsburg; Karlštejn |
| +1478 | total | +1095 | −725 | Salamanca |
| +1485 | total | +520 | −215 | Bourges; Fribourg |
| +1502 | partial | — | −125 | Kraków |
| +1539 | total | +2345 | −10 | Sevilla |
| +1598 | total | +245 | −360 | St Andrews; Edinburgh |

The result for +1239 in table 2 supersedes that in table 1, because we deem the report of the eclipse from Cerrato (table 2) to be more reliable than that of Cardeña (table 1; see discussion in the electronic supplementary material, p. 9).

## 5. Collected values of $\Delta T$ −720 to +2019 and long-term parabolic trend

The values of $\Delta T$ for the untimed and timed pre-telescopic data for −720 to +1600 are taken from [1, tables S1–S14]. Tables S10 and S11 of that paper are updated and supplemented by the results in tables 1 and 2. These changes are collected in electronic supplementary material, tables S2 and S3. The results are plotted in figure 1.

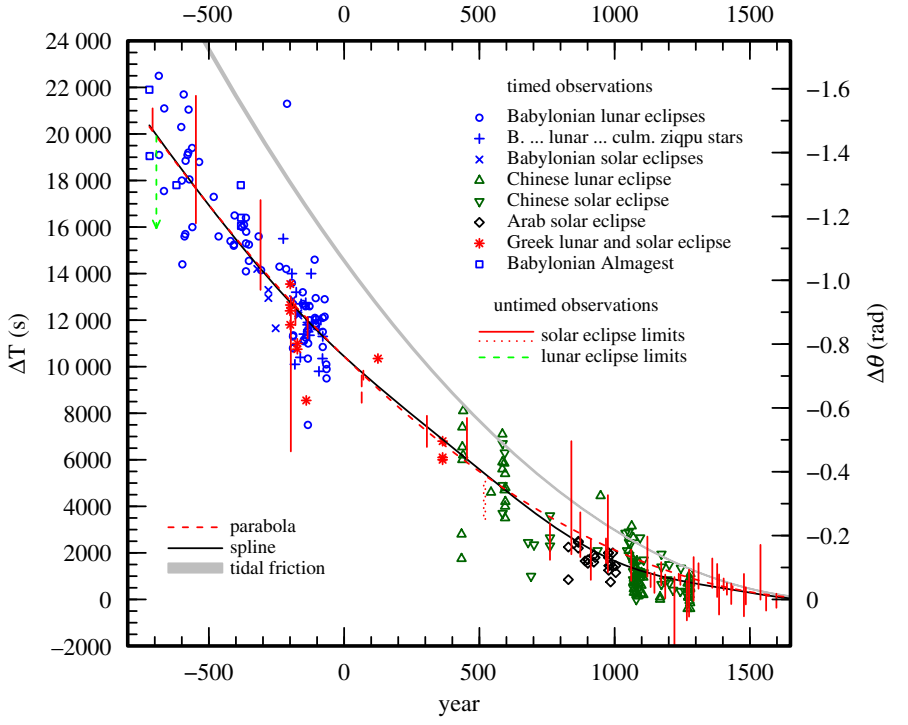


**Figure 1.** Collected results for $\Delta$T in the period $-720$ to $+1600$. The dashed curve is the long-term parabola, equation (5.1). The solid black curve is the spline fitted to all the data. The grey curve is the parabola, equation (5.2). The right-hand axis shows the sidereal rotational displacement angle of the Greenwich meridian, $\Delta\theta$ (rad), where the conversion factor is $\Delta\theta(\text{rad}) = -7.29 \times 10^{-5}\ \Delta\text{T (s)}$. (Online version in colour.)

In figure 1, there is a clear long-term parabolic trend in $\Delta$T demarcated independently by the timed and untimed observations of solar and lunar eclipses. This parabola is expressed by

$$\Delta\text{T} = -10 + (31.4 \pm 0.6)\left(\frac{\text{year} - 1825}{100}\right)^2 \text{s}. \tag{5.1}$$

It corresponds to a deceleration in the Earth's rate of rotation of $-4.59 \pm 0.08 \times 10^{-22}\ \text{rad s}^{-2}$ and a secular increase in the lod of $+1.72 \pm 0.03\ \text{ms cy}^{-1}$. The predicted parabolic change due to tidal friction, corresponding to a secular increase in the lod of $+2.40 \pm 0.01\ \text{ms cy}^{-1}$ [5], is

$$\Delta\text{T(tidal)} = +(43.7 \pm 0.2)\left(\frac{\text{year} - 1825}{100}\right)^2 \text{s}, \tag{5.2}$$

which is equivalent to a deceleration of $-6.39 \pm 0.03 \times 10^{-22}\ \text{rad s}^{-2}$. The difference between these decelerations reveals a non-tidal accelerative component in the Earth's rotation of $+1.8 \pm 0.1 \times 10^{-22}\ \text{rad s}^{-2}$ over the past 2700 years.

## 6. Spline fit to the values of $\Delta$T

Subtraction of the long-term parabolic curve (equation (5.1)) from the values of $\Delta$T allows a closer examination of the critical limits imposed by the untimed solar eclipses prior to $+1600$. These differences, $\delta(\Delta\text{T})$, within the range $\pm 2000$ seconds, are plotted in figure 2. The telescopic results after $+1600$, which are derived from timings of lunar occultations, are taken from our 2016 paper [1]. We note the relative smoothness on a centennial scale of the behaviour of $\delta(\Delta\text{T})$ after $+1600$,

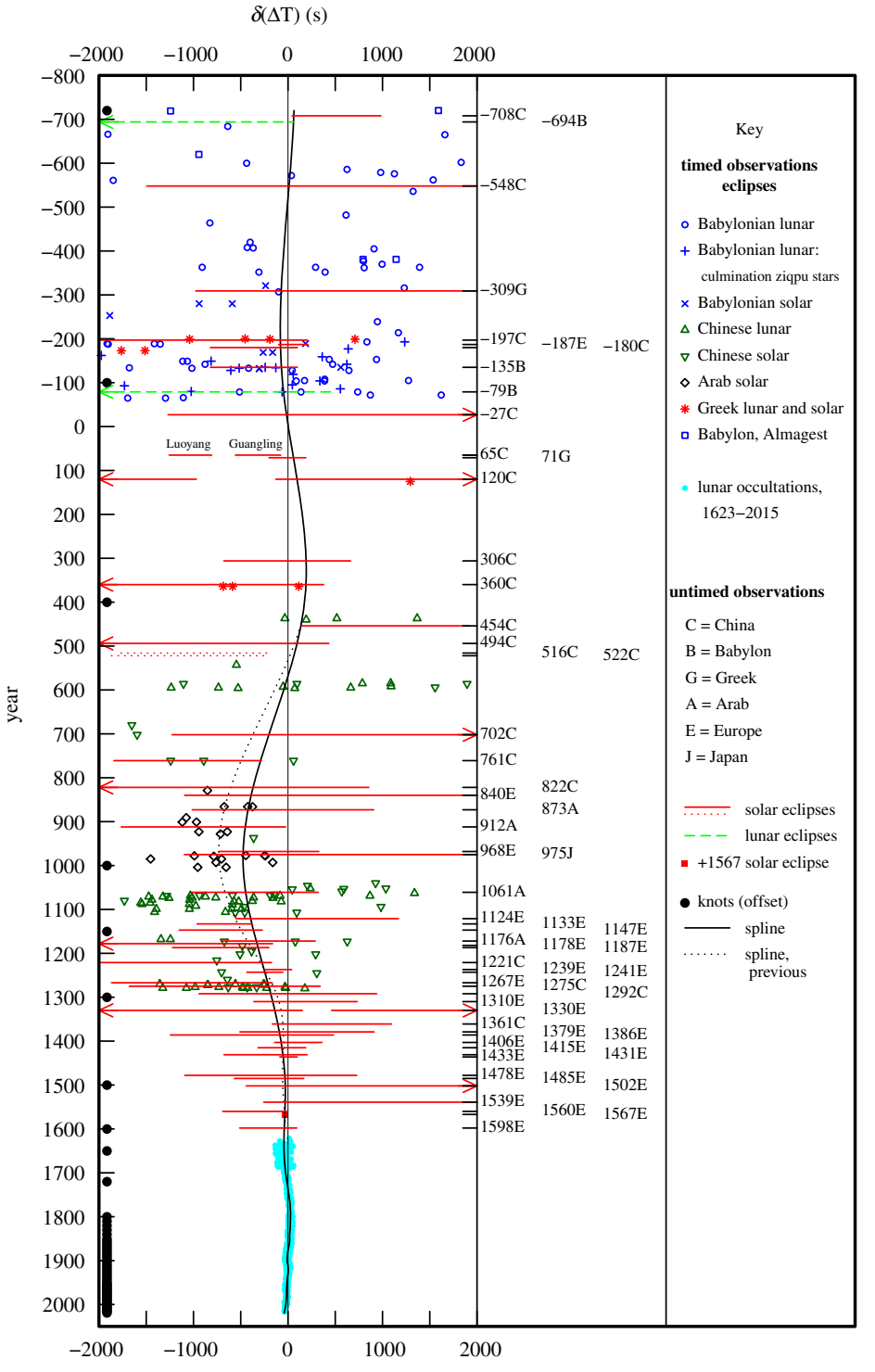


**Figure 2.** Plot of the differences $\delta\Delta T$ with respect to the parabola, equation (5.1), which is represented as a straight line at 0. The data after +1600 are derived from timings of lunar occultations, which are taken unaltered from our 2016 paper [1]. The solid black curve is the spline shown in figure 1, and the dotted curve in the period +800 to +1000 is the departure of the spline required to accommodate the timed Arab data in that period. The positions of the knots used in the spline fit are shown as black dots along the time axis. A higher resolution of the congested period +800 to +1660 is plotted in figure 3. (Online version in colour.)

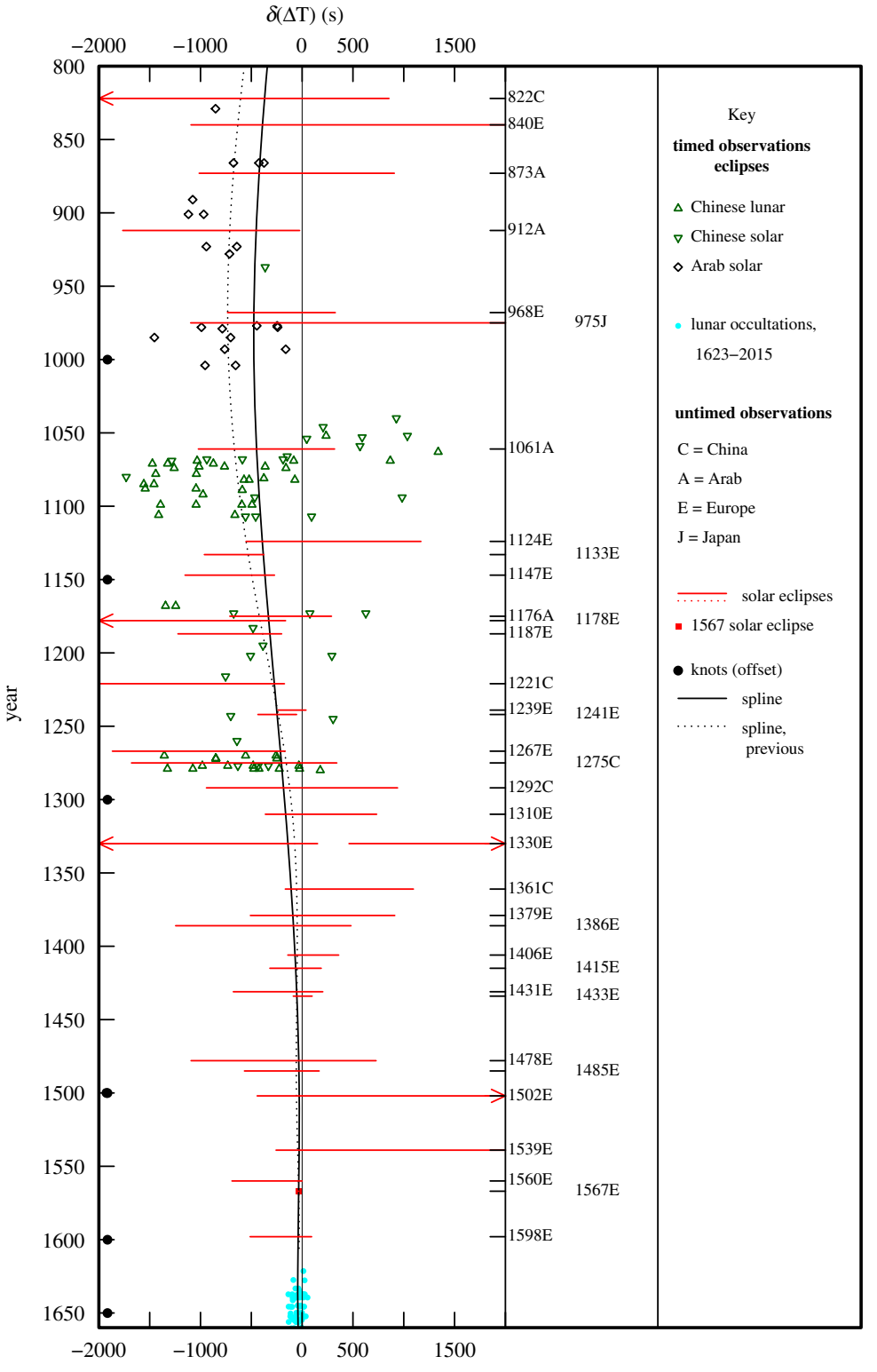


**Figure 3.** Plot of the differences $\delta\ \Delta$T in the period +800 to +1660 with respect to the parabola, equation (5.1), which is represented as a straight line at 0. The solid black curve is the spline shown in figure 1, and the dotted curve is the departure of the spline required to accommodate the timed Arab data in the period +800 to +1000. The positions of the knots used in the spline fit are shown as black dots along the time axis. (Online version in colour.)

**Table 3.** Critical eclipse limits in the fitting of the spline.

| year | $\Delta$T(s) | $\delta\Delta$T(s) |
|---|---|---|
| −708 | $< +20\,160$ | $< +40$ |
| −548 | $= +17\,660$[a] | $= +5$ |
| −187 | $+12\,590 < \Delta T < +12\,900$ | $-100 < \delta(\Delta T) < +210$ |
| −135 | $< +12\,140$ | $< +100$ |
| +71 | $< +9830$ | $< +190$ |
| +360 | $< +7100$ | $< +380$ |
| +454 | $> +6030$ | $> +140$ |
| +1124 | $> +980$ | $> -550$ |
| +1133 | $< +1160$ | $< -330$ |
| +1147 | $< +1160$ | $< -270$ |
| +1221 | $< +960$ | $< -175$ |
| +1239 | $> +830$ | $> -240$ |
| +1267 | $< +800$ | $< -165$ |
| +1361 | $> +500$ | $> -165$ |
| +1433 | $+385 < \Delta T < +570$ | $-85 < \delta(\Delta T) < +100$ |
| +1560 | $< +210$ | $< 0$ |
| +1567 | $+145 < \Delta T < +165$ | $-55 < \delta(\Delta T) < -35$ |
| +1598 | $< +245$ | $< +95$ |

Note: $\Delta$T and $\delta\Delta$T rounded to the nearest 10 or 5 s.

[a]See text.

and use this as a guide in fitting cubic splines to the data before +1600. The spacing of the knots (shown as dots along the time axis of figure 2) are chosen to reflect this, especially before +800, where there are fewer tight constraints on the behaviour of $\Delta$T.

Our new analysis of European solar eclipses has introduced a greater density of results after +1100. In figure 3, we reproduce the period +800 to +1660 on a greater scale in order to review the critical limits on $\delta(\Delta T)$ in that period. All the critical limits are listed in table 3.

These constraints on $\Delta$T are given high weight in the fitting of the cubic splines to all the data plotted in figures 1 and 2. The eclipse of −548 is assigned high weight at the point where it intersects the long-term parabola (5.1) in order to constrain the fluctuation of $\Delta$T around that epoch, where the data points have a relatively low density and high scatter. The only firm constraint before that epoch is the pincer-like limits set by the solar eclipse of −708 and the lunar eclipse of −694. The eclipse of −187 also sets relatively tight bounds at this early period. To reflect this an extra knot is added to those of the 2016 paper at epoch −100. Also, extra knots are added at +1150 and +1300 because of the increased number of observations in the medieval period.

The spline shown in figures 2 and 3 satisfies all the untimed constraints in table 3. The polynomial coefficients that represent this spline approximation are tabulated in electronic supplementary material, table S5.

It is noted from figures 2 and 3 that the mean of the relatively compact timed Arab solar eclipses between the epochs +800 and +1000 is offset from the spline curve. An exploratory spline fit, which is forced through the timed Arab data as well as the untimed limits, is shown as a dotted curve in figures 2 and 3. This has an impact on the change in the length of the day, which is derived from the time derivative of $\Delta$T. Before we consider the change in the length of the day, we assess the reliability of the Arab timed data.

## 7. Arab timings of solar eclipses in the period +800 to +1000

The timings were made with the unaided eye of the first and last contacts (1 and 4) of solar eclipses, where the image was either reflected in water or viewed through a filter to reduce the glare. The time of maximum eclipse was also estimated for some eclipses. The technique used in their estimation was different from the timings of the contacts, and we do not consider these further. The timings were made in local apparent time by measuring the altitude of the Sun with an astrolabe.

The mean of the timed Arab solar data is about 4 min (240 s) less than the solid spline in figures 2 and 3. A reduction in $\Delta$T (= TT − UT) means that the UT of the observation is greater than predicted, and hence the timings are systematically late by about 4 min. It is very likely that contact 1 was observed late because the incipient indentation of the Sun is not capable of resolution by the unaided eye, especially considering the glare of the Sun. On the other hand, by the same token, one might expect a systematic anticipation of the end of the eclipse (contact 4), and hence values of $\Delta$T greater than the spline. In general, this does not appear to be the case. The implication is that the observers delayed timing until they were sure that the eclipse had ended. From these arguments, we conclude that the timings of contacts 1 and 4 were probably subject to systematic errors of several minutes, and that the exploratory spline fit is dubious. If the observer had happened to be in the path of totality, the timing of the start and end of totality (contacts 2 and 3) would not have been subject to this error because these events are very sharp.

The aforesaid discussion also applies to the timing of the Chinese solar and lunar eclipses between +1000 and +1300. However, their dispersion in $\Delta$T is considerably greater than the Arab timings, and for that reason they provide less compelling evidence for adjustment of the spline.

## 8. Change in the length of the day

The time derivative of $\Delta$T measures the change in lod relative to the standard of 86 400 s SI. This is plotted in milliseconds (ms) in figure 4. The right-hand axis is the equivalent change in angular spin given by the relation $\Delta\omega(\text{rad s}^{-1}) = -0.843 \times 10^{-12}$ lod (ms). The difference between the average observed increase in the lod and that predicted on the basis of tidal friction reveals a non-tidal decrease of $-0.7$ ms cy$^{-1}$.

There are clearly fluctuations on a time scale of centuries in the lod. There can be no doubt of this given the combined evidence of the many eclipses after +500 displayed in figure 2. The well-known decadal fluctuations are resolved in the telescopic data after +1600. In the pre-telescopic period, the data are generally not precise enough to resolve changes less than on a centennial scale. However, there is evidence around +1500 for a departure from a smooth oscillatory variation on a centennial scale. Besides the average change in the lod of +1.72 ms cy$^{-1}$, which corresponds to a deceleration of $-4.59 \pm 0.08 \times 10^{-22}$ rad s$^{-2}$, the spline suggests a periodic fluctuation of $-3.5 \sin 2\pi t$ (ms), where $t = (\text{year} - 1750)/1400$.

In figure 4, we also include the result of fitting the exploratory spline which is forced to fit the timed Arab data in the period +800 to +1000. It is shown as a dotted curve in figure 4. This exaggerates the amplitude of the variation in the lod around +1200, and brings the general outline of the lod closer to that published in [1, fig. 18]. As argued in §7, we are now of the opinion that the timed eclipse data are biased, and we believe the centennial fluctuations displayed by the solid curve in figure 4 are an improvement over those in our 2016 paper [1].

## 9. Conclusion

The results for the changes in the Earth's spin on a centennial and longer time scale are displayed in table 4. The actual measured fluctuations in rate are plotted in figure 4 and can be obtained from electronic supplementary material, table S6.

The new and revised data in this addendum to our 2016 paper [1] have allowed us to modify and improve on the reliability of the results in that paper. The observed deceleration in the Earth's

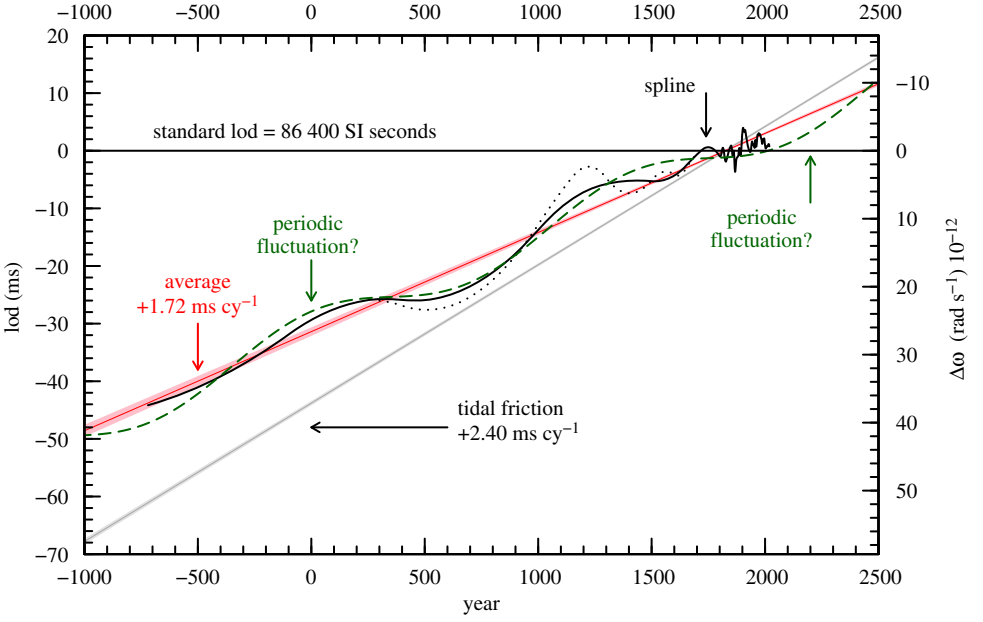


**Figure 4.** Variations in the lod (solid black curve), derived from the first time derivative along the spline shown in figures 2 and 3. The faint dotted curve between +500 and +1600 is the result of forcing the spline through the Arab timed data. The narrower shaded strip (pink) with uncertainty bandwidth is the observed deceleration, and the grey strip is the deceleration expected on the basis of tidal friction. The dashed curve is the speculative fluctuation with a period of 14 centuries. (Online version in colour.)

**Table 4.** Summary of the results for the Earth's spin.

| | length of day | SI units |
|---|---|---|
| deceleration | | |
| observed | $+1.72 \pm 0.03$ ms cy$^{-1}$ | $-4.59 \pm 0.08 \times 10^{-22}$ rad s$^{-2}$ |
| tidal | $+2.40 \pm 0.01$ ms cy$^{-1}$ | $-6.39 \pm 0.03 \times 10^{-22}$ rad s$^{-2}$ |
| deduced acceleration | $-0.7 \pm 0.1$ ms cy$^{-1}$ | $+1.8 \pm 0.1 \times 10^{-22}$ rad s$^{-2}$ |
| conjectured periodic fluctuation in rate, where $t =$ (year $-$ 1750)/1400 | $-3.5 \sin 2\pi t$ ms | $+3.0 \sin 2\pi t \times 10^{-12}$ rad s$^{-1}$ |

spin is significantly less than that predicted by tidal friction. The densification of our dataset in the period AD 800–1600 supports our conclusion in the 2016 paper that there is a fluctuation in the rate of spin on a centennial time scale. However, there are not enough reports of critical eclipse observations before 136 BC to determine whether this fluctuation is truly part of a periodic term of about 14 centuries.

Data accessibility. Web pages are available from HM Nautical Almanac Office's website at http://astro.ukho.gov.uk/nao/lvm; these contain the observational data, polynomials that represent the spline fit as well as tables of lod and ΔT at various intervals, together with estimates of their errors and related material.

Authors' contributions. L.V.M. carried out the analysis of the values of ΔT; M.Z. collected the eclipse records; F.R.S. provided the estimation of the eclipse records; and C.Y.H. obtained, wrote and ran the computer programs to produce the results and the figures. All authors contributed to writing/revising the paper, approved the final version and agree to be held accountable for all aspects of the work.

Competing interests. We declare we have no competing interests.

Funding. We received no funding for this study.

Acknowledgements. The authors thank Steve Bell of HM Nautical Almanac Office and the UK Hydrographic Office for hosting the web pages.

## References

1. Stephenson FR, Morrison LV, Hohenkerk CY. 2016 Measurement of the Earth's rotation: 720 BC to AD 2015. *Proc. R. Soc. A* **472**, 20160404 (doi:10.1098/rspa.2016.0404)
2. Morrison LV, Stephenson FR, Hohenkerk CY. 2020 Historical changes in UT/LOD from eclipses. See https://web.ua.es/journees2017/proceedings/PROCEEDINGS-JOURNEES.pdf.
3. Stephenson FR, Morrison LV, Hohenkerk CY. 2018 The provenance of early Chinese records of large solar eclipses and the determination of the Earth's rotation. *J. Hist. Astr* **49**, 425–471. (doi:10.1177/0021828618789850)
4. Morrison LV, Stephenson FR, Hohenkerk CY. 2019 Rome and the total solar eclipse of BC 188 July 17. *J. Hist. Astron.* **50**, 366–372. (doi:10.1177/0021828619863243)
5. Williams JG, Boggs DH. 2016 Secular tidal changes in lunar orbit and Earth rotation. *Celestial Mech. Dyn. Astron.* **126**, 89–129. (doi:10.1007/s10569-016-9702-3)